Cancer Cell International

RESEARCH

Open Access

Wee1 inhibitor PD0166285 sensitized TP53 mutant lung squamous cell carcinoma to cisplatin via STAT1

Qi Li[1,2†], Wenjie Yang[3†], Qingyi Zhang[4†], Daoming Zhang[5†], Jun Deng[6], Binxin Chen[1,2], Ping Li[2], Huanqi Zhang[5], Yiming Jiang[5], Yangling Li[2,5], Bo Zhang[7,8*] and Nengming Lin[1,2*]

Abstract

Background Lung squamous cell carcinoma (LUSCs) is associated with high mortality (20–30%) and lacks of effective treatments. Almost all LUSC exhibit somatic mutations in *TP53*. Wee1, a tyrosine kinase, regulates the cell cycle at the G2/M checkpoint. In TP53-deficient cells, the dependence on G2/M checkpoints increases. PD0166285 is the first reported drug with inhibitory activity against both Wee1 and PKMYT1.

Methods Protein expression was determined by Western blot analysis. Cell proliferation was assessed using cell colony formation and CCK-8 assays. Cell cycle was performed by PI staining with flow cytometry. Apoptosis was evaluated using Annexin V-Phycoerythrin double staining and flow cytometry. DNA damage was detected through comet assay and immunofluorescence assay. In vivo, apoptosis and anti-tumor effects were assessed using the TUNEL assay, a nude mouse model, and immunohistochemistry (IHC). Co-immunoprecipitation assay was used to detect protein–protein interactions. We analyzed Wee1, PKMYT1, and Stat1 expression in pan-cancer studies using the Ualcan public database and assessed their prognostic implications with Kaplan–Meier curves.

Result PD0166285, a Wee1 inhibitor, effectively inhibits Wee1 activity, promoting cell entry into a mitotic crisis. Moreover, PD0166285 sensitizes cells to cisplatin, enhancing clinical outcomes. Our study demonstrated that PD016628 regulates the cell cycle through Rad51 and results in cell cycle arrest at the G2/M phase. We observed increased apoptosis in tumor cells treated with PD0166285, particularly when combined with cisplatin, indicating an enhanced apoptotic response. The upregulation of γ-H2AX serves as an indicator of mitotic catastrophe. Co-immunoprecipitation and data analysis revealed that apoptosis in LUSC is mediated through the Stat1 pathway, accompanied by decreased levels of Socs3. Furthermore, IHC staining confirmed significant differences in the expression of Phospho-CDK1 and γ-H2AX in LUSCs, suggesting involvement in DNA damage.

Conclusions In summary, our study suggests that PD0166285, an inhibitor of Wee1, sensitizes LUSC cells to cisplatin and modulates DNA damage and apoptosis pathways through Rad51 and Stat1, respectively. These findings highlight the combination of PD0166285 and cisplatin as a promising therapeutic approach for treating LUSC.

Keywords PD0166285, Wee1 inhibitor, Lung squamous cell carcinoma, Stat1, Cell cycle

†Qi Li, Wenjie Yang, Qingyi Zhang and Daoming Zhang have contributed equally to this work.

*Correspondence:
Bo Zhang
zhangbo1009@zju.edu.cn
Nengming Lin
lnm1013@zju.edu.cn
Full list of author information is available at the end of the article

Introduction

Lung cancer is a leading cause of cancer-related mortality worldwide, resulting in 1.8 million deaths in 2020 [1–3]. Approximately 80% of cases classified as non-small cell lung cancer (NSCLC), include lung adenocarcinoma (LUAD) and lung squamous cell carcinoma (LUSC) two subtypes [1, 2]. Around 20%-30% of NSCLC diseases belong to the lung squamous cell carcinoma (LUSC) subtype [1, 4]. Unlike LUAD, patients with LUSC have not experienced similar benefits from targeted therapies.. Despite breakthroughs in early diagnosis and cancer treatments for lung cancer patients, LUSC are still associated with high mortality and a lack of therapies specific to this disease [5, 6]. Still, platinum-based chemotherapy remains the cornerstone of the current treatment for LUSCs [5].

Since tumor growth is largely driven by cell cycle checkpoints and DNA damage response (DDR) processes, we investigate the responsible signaling pathways as potential targets for LUSC therapy [7–9]. Wee1 and PKMYT1 are considered potential candidates within the Wee1 kinase family for targeted cancer therapies [10]. Wee1 and PKMYT1 kinases at the G2-M phase are membrane-associated tyrosine- and threonine-specific cdc2-inhibitory kinases, which play critical roles at the G2-M cell cycle checkpoint [10, 11]. Wee1 can phosphorylate cyclin-dependent kinase 1 (CDK1) on phospho-CDK1 (Tyr15), and PKMYT1 can activate both on Tyr15 and Thr14 [12]. Inhibition of Wee1 kinase causes a significant reduction in Tyr15 levels, which in turn promotes the accumulation of the active CDK1/Cyclin B1 complex, thereby facilitating mitotic entry [13]. Inhibition of Wee1 and PKMYT1 kinases leads to the override of the G2/M cell cycle checkpoint, resulting in premature entry into mitosis and subsequent cell death during mitosis. This process is commonly referred to as mitotic catastrophe [10].

Cells expressing wild-type *TP53* arrest at the G1 checkpoint to be able to repair damaged DNA [14, 15]. Tumor cells that typically lack *TP53* are dependent on the G2 checkpoint to repair DNA damage [6]. Thus, targeting the G2 checkpoint in *TP53*-deficient tumor cells is a promising therapeutic avenue [16, 17]. Inhibition of Wee1, can abolish the G2 checkpoint and therefore lead to cell death [18, 19].

LUSC tumor cells frequently harbor mutations in the *TP53, CDKN2A, PTEN, PIK3CA, KEAP1, MLL2, HLA-A, NFE2L2, NOTCH1*, and *RB1* genes [1, 20]. A majority of LUSCs exhibit somatic mutations in the *TP53* gene [20–22]. The inhibition of Wee1 has been shown to augment the efficacy of cisplatin, thereby improving clinical outcomes in cancer patients, albeit with mechanisms not fully elucidated for all compounds [14, 23]. Several small-molecule inhibitors of Wee1 have been developed, including AZD-1775, PD0166285, and PD0407824. Among these, PD0166285, a co-inhibitor of Wee1 and Myt1, has demonstrated effectiveness across a spectrum of cancers including cervical cancer, colon cancer, lung cancer, melanoma, ovarian cancer, esophageal squamous cell carcinoma, hepatocellular carcinoma, as well as in glioblastoma cell lines and xenografts [24–27]. AZD-1775 is currently in the clinical trial phase to determine its efficacy against tumors with high Wee1 expression. However, AZD1775 exerts its single-agent cytotoxicity not only by inhibiting Wee1 but also by interacting with additional targets, independent of *TP53* status [28]. Common adverse events associated with Wee1 inhibitors include hematologic events, nausea, vomiting, and fatigue [27]. Numerous studies have reported that PD0166285 exhibits enhanced sensitivity specifically in TP53-mutated cancers compared to other Wee1 inhibitors [10, 29]. Currently, Wee1 inhibitors are recognized as chemosensitizing agents, with numerous studies demonstrating their synergistic activity with DNA-damaging agents in preclinical models [10, 30, 31]. On the other hand, platinum agents were among the initial agents tested in phase I trials in combination with Wee1 inhibitors [32]. While, the research investigating the combination of PD0166285 with cisplatin in LUSC remains unclear.

Stat1 is a pivotal transcription factor belonging to the Signal Transducer and Activator of Transcription (Stat) protein family. It plays integral roles in various cellular functions, such as proliferation, differentiation, migration, apoptosis, homeostasis, immune signaling, and immune response [33, 34]. Stat1 is implicated in the pathogenesis of pancreatic cancer, breast cancer, osteosarcoma, and small cell lung cancers (SCLCs) [34–36]. Triparna Sen and Hui Wen Lo et al. cl have indicated that inhibiting Wee1 could affect the JAK/Stat signaling and STING pathways in breast cancer and SCLCs [34, 37]. Due to the anti-tumor effect of Stat1, it has been identified as a therapeutic target [33]. Another study demonstrated that treatment with AZD1775 significantly increased Stat1 phosphorylation [37]. However, the relationship between Wee1 and Stat1 remains unclear.

Thus, in the current study, we investigated that Wee1 as a promising therapeutic target in LUSC. We discovered that PD0166285 in combination with cisplatin can inhibit the growth of LUSCs and promote apoptosis. Moreover, we elucidated the relationship between Wee1 and Stat1 and identified potential mechanisms by which Wee1 mediates chemo-sensitization to cisplatin in LUSC.

Materials and methods

Cell culture and drugs

The human lung bronchus epithelial cell lines BEAS-2B, A549, H226, H520 and Calu1 cell lines were cultured at 37 ℃ with 5% CO2 in 90% DMEM (HyClone, USA) or RPMI1640 medium (HyClone, USA) supplemented with 10% fetal bovine serum (HyClone, US) and 1% penicillin/streptomycin (Life Technologies, Grand Island, NY). All cell lines were obtained from the Shanghai Institute of Biochemistry and Cell Biology (Shanghai, China). Cisplatin (HY-17394) and PD0166258 (HY-13925) were obtained from MedChemExpress (MCE, America), dissolved in dimethyl formamide (DMF) and dimethyl sulfoxide (DMSO) (Sigma), respectively, and added to the medium at a final concentration of up to 0.1% DMF/DMSO.

Western blot analysis

The cells were inoculated in 6-well plates at a density of 2×10^5 cells per well and lysed with RIPA buffer (Beyotime, China) supplemented with 1× protease inhibitor (Solarbio, China) and phosphatase inhibitor (Solarbio, China). Then the bicinchoninic acid (BCA) protein detection kit (Thermo, USA) was used to determine the protein concentration. The proteins were denatured by boiling in 1.5× SDS loading buffer. Equal amounts of proteins were separated by SDS-PAGE and transferred to NC membranes. 5% non-fat milk was used to block the membranes at room temperature, and then the membranes were incubated overnight at 4 °C with primary antibodies. After washing in Tris-buffered saline containing Tween 20 (TBST), the membranes were incubated with secondary antibodies at room temperature for 1 h. The membrane were washed and ECL reagent, before analyzing with the Bio-Rad molecular Imager ChemiDoc XRS + system (BioRad, USA).

ATM (#2873), phospho-H2AX (S139, #9718), Wee1 (#13084S), CyclinB (#12231t), Phospho-CDK1 T14 (#AP1465), Phospho-CDK1 Y15 (#ab76146), β-Actin (#EM2001-07), PARP (#9532s), Cleaved PARP (#5625s), Caspase 3 (#9662s), Cleaved Caspase 3 (#9661s), Caspase 9 (#ab202068), Bcl-2 (#3498S), Bcl-XL (2764S), Mre11 (#4847T), Rad51 (#ab133534), Rad50 (#3427T), Stat1 (#14994S), Phospho-Stat1 (#9167S), Socs3 (#2932s) primary antibodies as well as anti-rabbit (#7074) and anti-mouse (#7076) secondary antibodies were purchased from Cell Signaling Technology (Danvers, MA), Abclonal (Wuhan, China), Huabio (Hangzhou, China), and Abcam (Cambridge, UK).

Cell viability assay

The cells were seeded into 96-well plates at a density of 3500 cells per well and incubated overnight in complete medium. Following drug treatment for 48 h, cell viability was measured using Cell Counting Assay Kit-8 (CCK8) (MCE, USA) and measured with a microplate reader (BioRad, USA) at an absorbance of 450 nm. All experiments were repeated three times.

Colony formation assay

The efficacy of PD0166285 combined with cisplatin was assessed using clonogenic assays. Briefly, the cells were incubated in 6-well plates and treated with various drugs for 2 weeks until visible colonies formed. Cells were fixed with 4% paraformaldehyde (PFA, Solarbio, Beijing, China) for 15 min, and then stained with 0.1% crystal violet for 20 min at room temperature. After washing with PBS, colonies consisting more than 50 cells were counted using ImageJ software. Each experiment was conducted in triplicate.

Cell cycle assay

After exposure to PD0166258 with or without cisplatin for 48 hours, the cells were harvested, washed three times with PBS, fixed in 70% prepared pre-cooled ethanol, and incubated overnight at − 20 ℃. After washing with PBS three times, the cells were stained with propidium iodide (PI)/RNase solutions using a commercial cell cycle detection kit (BD Biosciences) at room temperature for 15 minutes in the dark. The stained cells were then analyzed using BD FACS Canto II (BD Biosciences) within 1 hour. Data analysis was performed using ModFit LT version 5.0 software (Verity Software House, Topsham, ME). All assays were performed three times.

Cell apoptosis assay

The cells were cultivated in 6-well plates, and treated with cisplatin, PD0166285, and PD0166285 combined with cisplatin for 48 hours. Then all the samples were washed in PBS, and double-stained using the Annexin V-Phycoerythrin (PE) kit and the FITC apoptosis detection kit (BD Biosciences, Erembodegem, Belgium) for 30 minutes. Apoptotic cells were detected by flow cytometry within 1 h (BD Biosciences), and the results were analyzed using the FlowJo version 10.8.1 software (FlowJo, Oregon). All assays were performed three times.

Immunofluorescence staining assay

Cells at a density of approximately 10,000 cells/ml were seeded on a 14 mm glass slides in 24-well plates (NEST, Jiangsu, China) and incubated overnight. Then the samples were treated with respective compounds. Subsequently, the cells were immobilized with 4% PFA for 10 minutes, followed by permeabilized with 0.5% Triton X-100 (Amresco, Solon, OH) for 20 minutes and blocked with 5% bull serum albumin (BSA) (A8020,

Solarbio,Beijing, China) at room temperature for 30 minutes. Then the primary antibody against γH2AX (1:100) was stained overnight at 4 °C. After that, cells were incubated with Alexa Fluor 488-conjugated goat anti-rabbit immunoglobulin G (IgG) (Molecular Probes, Eugene, OR, 1:100) in the dark for 30 minutes at room temperature. Finally, Hoechst (Beyotime, Jiangsu, China, 1:3,000) was used for stained in the dark for 5 minutes. Images were captured with the Leica TCS SP8 confocal microscope. All samples were washed with PBS and all images were acquired using the same exposure parameters.

siRNA transfection

For protein knockdown, NCI-H226 and NCI-H520 cells were transfected with Jetprime Reagent (Polyplus-transfection, France) according to manufacturer's instructions, using final siRNA concentrations of 50 nM. The day after siRNA transfection, cells were re-seeded and incubated until 48 hours after transfection and collected for analysis. The siRNAs targeting Wee1 were synthesized by GenePharm (China). The sequences of siRNAs were as follows:

si wee1#1: GCAGCCAGGAAUAUGUUCUTT.
si wee1#2: GGCACAAGAAGAAUCAAGATT.
si wee1#1: GGCAAUAUGUCUAUUCUAAGGTT.

Comet assay

A comet assay kit (Trevizen, USA) was used to assess the DNA damage. A total of 2×10^4 cells were suspended in low-melting agarose and spread on a comet slide followed by solidification at 37 °C. Then the slides were immersed in the pre-cooled lysis buffer at 4 ℃, and then transferred to an alkaline solution (0.3 M NaOH, 1 mM EDTA) and neutralized in TBE buffer (Tris Base 108 g, Boric Acid 55 g, EDTA 9.3 g, ddH_2O 1 L). The slides were fixed in 70% ethyl alcohol and stained with SYBR Green I. All the images were captured by Olympus IX71 inverted microscope (Tokyo, Japan). The percentage of "tailed" DNA in at least 50 cells and the tail "moment" (TM = percentage of DNA in the tail × tail length) were measured using the CASP software, and at least 50 cells were counted.

Co-immunoprecipitation assay

The cells were inoculated in a 10 cm dish for the corresponding before lysis with NP-40 lysis buffer added with PMSF (1:1000) for 30 minutes and centrifuged at 12000 g at 4 ℃ for 10 minutes. Then the specific antibodies were added to the supernatant and the samples were incubated overnight at 4 ℃. The antibody-bound proteins were then incubated with protein A/G magnetic beads for 1 hour at 4 ℃. Subsequently, the beads were washed three times with washing buffer, with each wash lasting 5 minutes. The N beads were boiled with 1.5× loading buffer for western blot analysis.

Nude mouse model

Suspensions containing 5×1^6 cells in a 1:1 mixture of serum-free medium were injected into the flanks of 6-week-old female nude mice (Hangzhou Medical College Experimental Animal Center, Hangzhou, China). Once the mean tumor volume reached approximately 100–150 mm^3, the mice were randomly assigned to four groups of six in each group, and each group received a different treatment (normal saline, cisplatin, PD0166285, and PD0166285+cisplatin). The size of the tumors was measured every 2 days using calipers and volumes were calculated using the formula: $width^2 \times length \times 0.5$. After 2 weeks of treatment, the mice were sacrificed, and tumors, livers, and kidneys were collected for subsequent experiments.

Immunohistochemistry (IHC) assay

Tissues were fixed with formalin, embedded in paraffin, and cut into 4 mm sections. Then the slides were dewaxed in xylene and dehydrated in graded alcohols. Antigen retrieval was performed by boiling the slides in 10 mM citrate buffer using a microwave for 20 minutes, followed by cooling to room temperature for 2 h. After treating with 3% H_2O_2 and 5% goat serum, all samples were incubated with primary anti-phos-CDK1 Y15 (1:100) and γH2AX (1:100) overnight at 4℃. After the sections were washed with PBS, they were incubated with secondary biotinylated antibody and DAB stain (GeneTech. USA). Images were captured using a Motic EasyScan microscope (Motic, USA).

Statistical analysis

Our results were expressed as the mean ± SD and analyzed using GraphPad Prism (GraphPad Software Inc, USA). Each experiment was conducted independently at least three times. The significance level was indicated as $^*p<0.05$, $^{**}p<0.01$, $^{***}p<0.001$.

Results

Wee1 inhibitor PD0166285 inhibited Wee1 and PKMYT1 activities in LUSC

We initially assessed the expression of Wee1 and PKMYT1 in human cancer using public databases. From the public database (UALCAN (uab.edu), we found that Wee1 and PKMYT1 were highly expressed in LUSCs (Fig. 1a). Expression of Wee1 and PKMYT1 in the database is associated with poor patient outcomes (Fig. 1b). Compared to pan-cancer tissues, cancer tissues exhibited significantly higher levels of Wee1 and PKMYT1 expression (Fig. 1c). Moreover, overexpression of Wee1 and

PKMYT1 was notably associated with TP53-mutated LUSCs (Fig. 1d).

To explore the therapeutic potential of PD0166285, NCI-H226, NCI-H520 and Calu1 cell lines were treated with different concentrations of PD0166285 (0 nM, 200 nM, 400 nM, 800 nM). PD0166285 treatment led to a significant decrease in both the number and size of cell colonies (Fig. 1e). The anti-tumor efficacy of PD0166285 was further assessed using the CCK8 assay. TP53-mutated LUSCs cells displayed differential responses to PD0166285 and cisplatin, with IC50 values for PD0166285 ranging from 641 to 1204 nM. Previous studies have shown that TP53-mutated cells are more sensitive to the Wee1 inhibitor [7, 10, 38]. The IC50 values of cisplatin in LUSCs ranged from 1.520 to 2.579 μM (Fig. 1f). Then NCI-H226, NCI-H520 cell lines were treated with 400 nM PD0166285 for various durations to examine the expression of Wee1, CyclinB, p-CDK T14 and p-CDK Y15. Our findings demonstrated a time-dependent inhibition of Wee1 and PKMYT1 at the protein level within 0-48 hours post-treatment with PD0166285 (Fig. 1g).

PD0166285 arrested LUSC cells at the G2–M phase of the cell cycle

To assess the impact of PD0166285 on mitosis in LUSCs, NCI-H226 and NCI-H520 cells were treated with varying concentrations of PD0166285 for 48 h (0 nM, 200 nM, 400 nM, 800 nM). Flow cytometry analysis revealed a significant decrease in the proportion of cells in the G2/M phase following treatment (Fig. 2a, b). Consistent with these findings, the expression levels of cell cycle-related proteins were also altered (Fig. 2c, d). Overall, our results suggest that PD0166285 inhibits the growth of LUSC cells by arresting them in the G2/M phase.

PD0166285 induces apoptosis in LUSC cells

To determine if treatment with PD0166285 and cisplatin triggered apoptosis in LUSC cells, Annexin-V staining was performed. As shown in the Fig.s, the proportion of apoptotic cells significantly increased in a dose-dependent manner (Fig. 3a, b), which was further corroborated by an increase in protein level (Fig. 3c).

PD0166285 augments the efficacy of cisplatin in LUSC cells by blocking the G2/M phase

PD0166285 demonstrated a dose-dependent effect on the proliferation of LUSC cells. To evaluate the effect of PD0166285 on cell proliferation, LUSC cells were treated with 400 nM of PD0166285 and 1 μM of cisplatin (Fig. 4a). Given that DNA damage is a prerequisite for Wee1 inhibitor efficacy, cells were pre-treated with cisplatin (1 μM) for four hours before adding PD0166285. After 14 days, the cells were fixed and stained with 0.1% crystal violet solution. The combination of cisplatin with PD0166285 showed significantly higher antiproliferative efficacy compared to monotherapy (Fig. 4b).

Cells deficient in TP53 are more dependent on G2/M checkpoints, and TP53 mutations are prevalent in LUSCs tumor cells. Therefore, we investigated the effect of PD0166285 in TP53 mutant cells. As expected, the anti-tumor effects of the PD0166285-cisplatin combination therapy were enhanced in TP53 mutant LUSC cells, as evidenced by both flow cytometry and protein analysis. We found that PD0166285 can arrest the cell cycle at the G2/M phase, and that the expression levels of p-CDK1 T14 and p-CDK1 Y15 were decreased in the combination treatment (Fig. 4c, d).

PD0166285 potentiates chemo-sensitization of cisplatin through induction of apoptosis

The combination of PD0166285 and cisplatin induced greater apoptosis compared to either compound alone (Fig. 5a). Western blot analysis further demonstrated that, compared to PARP, caspase3, and caspase9, the expression levels of their cleaved forms—cleaved-PARP, cleaved-caspase3, and cleaved-caspase9—were increased (Fig. 5b). These findings indicate that the combination therapy of PD0166285 and cisplatin significantly increases apoptosis in LUSC cells Interestingly, a similar significant effect, determined using TUNEL assay, was also observed in nude mice (Fig. 5c).

(See figure on next page.)

Fig. 1 Wee1 and PKMYT1 expression in LUSCs tissues at mRNA and protein levels. **a** Differential mRNA expression of Wee1 and PKMYT1 in pan-cancer analysis from TCGA data obtained from the UALCAN. Wee1 and PKMYT1 exhibit high expression levels in LUSCs. **b** Overall survival of patients with LUSCs after successful surgery. KM survival curves for overall survival in LUSC patients from the Kaplan–Meier plotter online database. Grouping by "auto select best cutoff". **c** Expression of Wee1 and PKMYT1 in LUSC tissues (TCGA, n = 503) compared to healthy lung tissues (TCGA, n = 52) assessed by RNASeq. **d** Western blot analysis of Wee1 and PKMYT1 expression in BEAS-2B cells, A549, Calu1, NCI-H226, and NCI-H520 cells. **e** Colony formation assay of LUSC cells treated with various concentrations (0 nM, 200 nM, 400 nM, and 800 nM) of PD0166285. **f** The CCK-8 assay revealing the IC50 values of PD0166285 and cisplatin in LUSCs. **g** Time-dependent inhibition of Wee1 and PKMYT1 by PD0166285 at different concentrations. *$p < 0.05$, **$p < 0.01$, ***$p < 0.001$

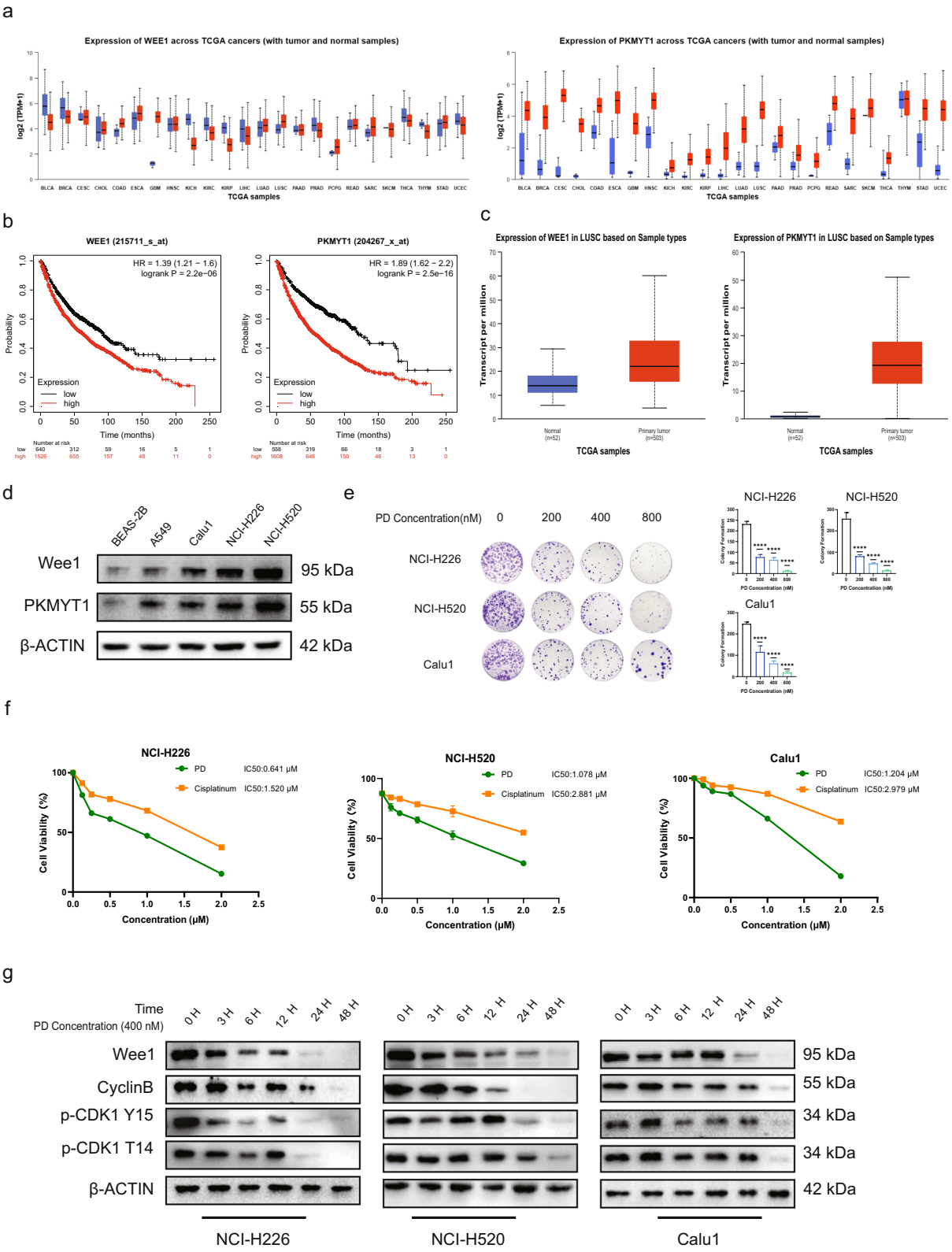

Fig. 1 (See legend on previous page.)

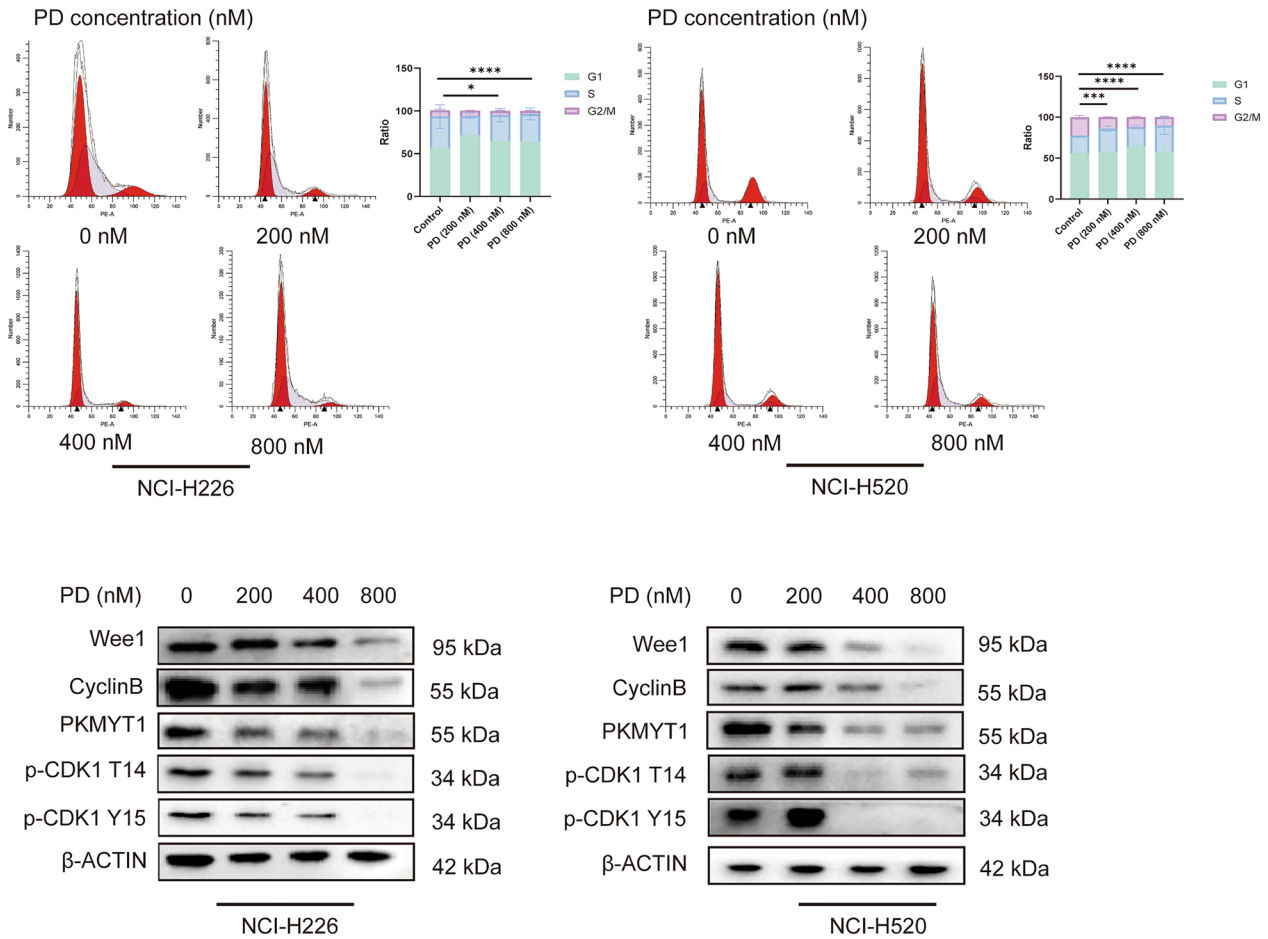

Fig. 2 PD0166285 blocks G2/M phase of the cell cycle in a dose-dependent manner. **a, b** Flow cytometry analysis showing PD0166285-induced blockade of G2/M phase in LUSCs. **c, d** Western blot analysis demonstrating PD0166285-mediated inhibition of the cell cycle-related proteins in LUSCs. *$p < 0.05$, **$p < 0.01$, ***$p < 0.001$

PD0166285 decreased the DNA damage level and attenuated DNA damage repair by inhibiting the function of Rad51

We found that PD0166285 attenuated the levels of γ-H2AX in NCI-H226 and NCI-H520 cells (Fig. 6a). Co-administration of cisplatin and PD0166285 resulted in elevated γ-H2AX expression, indicating activation of the Wee1-mediated DNA damage response, consistent with previous studies [39]. An alkaline comet assay was conducted to directly evaluate the effect of PD0166285 on DNA damage repair. As shown in Fig. 6b, following four hours of cisplatin treatment, combination with PD0166285 significantly increased the 'comet tail' length and tail moment, indicative of impaired DNA damage repair in LUSC cells.

To further explore the underlying mechanism of the DNA damage repair pathway, we examined relevant proteins (ATM, P95, MRE11, Rad50, Rad51, γ-H2AX). We found a down-regulation of Rad51 expression, with no significant changes in other proteins (Figs. 6c).

Stat1 interacts with Wee1 in LUSCs

Previous studies have indicated that cellular stress arising from DNA replication levels is associated with genomic instability and micronucleus formation. According to the TCGA database, Stat1 is highly expressed in cancers (Fig. 7a, b). To determine the effect of Stat1 expression on the survival of LUSC patients, we conducted a prognostic analysis using TCGA data. The Kaplan-Meier (KM) curve demonstrated a significant correlation between Stat1 expression and poorer overall survival (OS) in LUSC patients (Fig. 7c). Previous research has implicated Stat1 in apoptosis and our study also found that PD0166285 induces apoptosis. To explore the interaction of Stat1 and Wee1, we performed the co-immunoprecipitation assay, which showed that Stat1 and Wee1 interacted (Fig. 7d). We also observed that in the absence of Wee1,

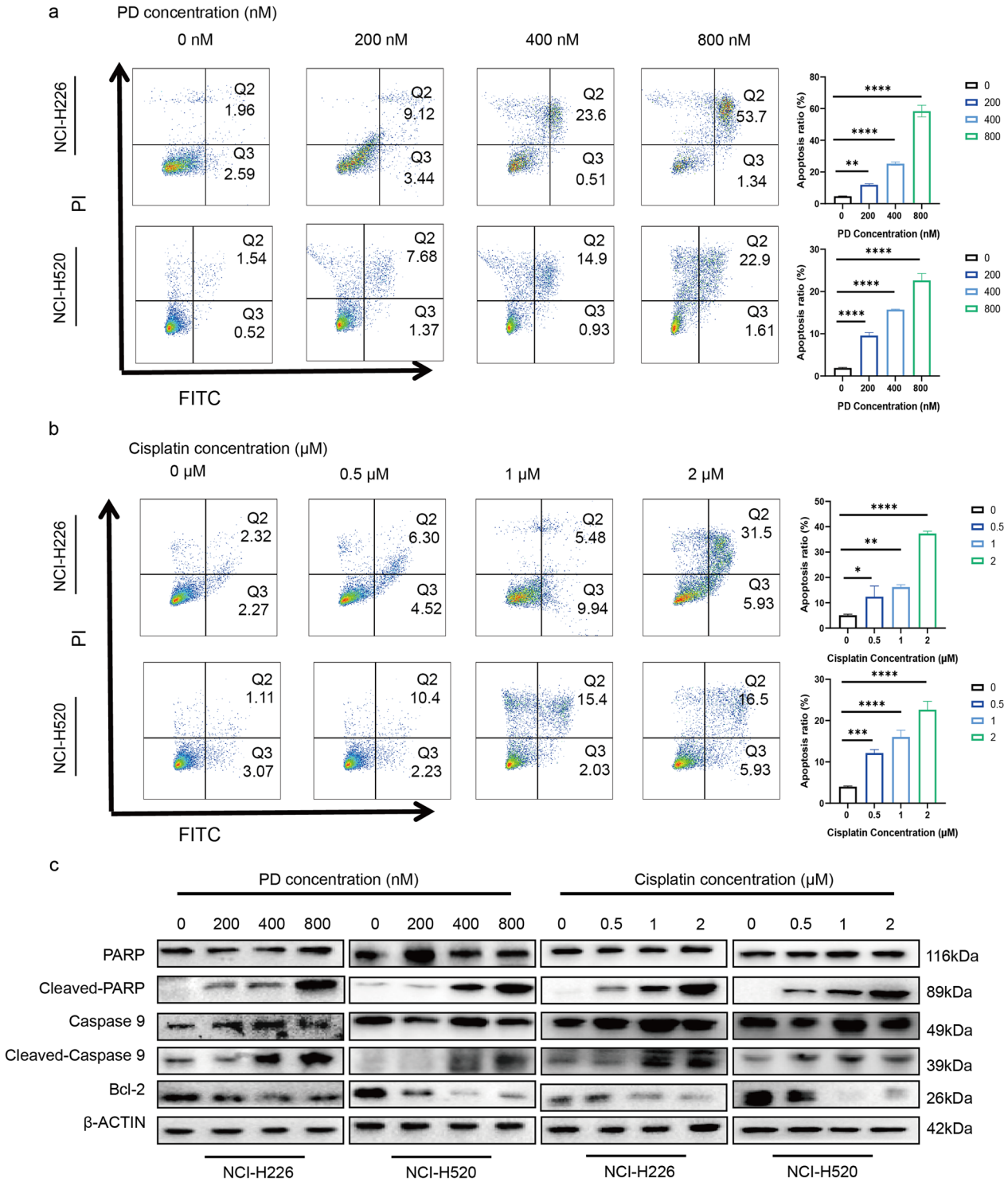

Fig. 3 PD0166285 and cisplatin induce apoptosis in a dose-dependent manner. **a, b** Flow cytometry analysis showing PD0166285 and cisplatin-induced apoptosis in LUSCs. **c** Western blot analysis of apoptotic proteins in the presence and absence of PD0166285 and cisplatin in LUSCs. *$p < 0.05$, **$p < 0.01$, ***$p < 0.001$

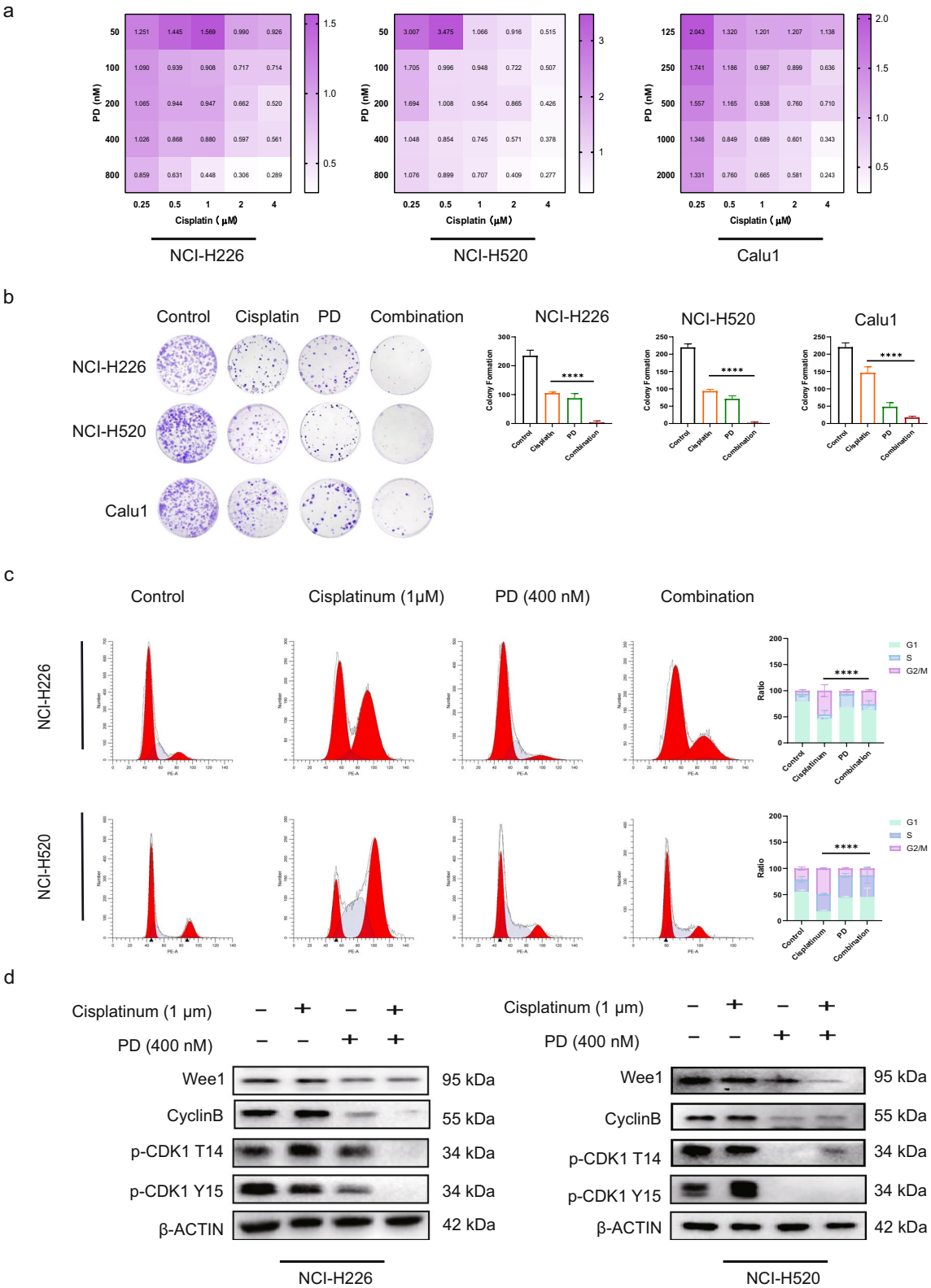

Fig. 4 PD0166285 sensitizes LUSC cancer cells to cisplatin. **a** Calculation of the combination index (CI) for PD0166285 and cisplatin treatment. **b** The inhibitory effect on colony formation following treatment with PD0166285 combined with cisplatin in LUSCs. **c** PD0166285 combined with cisplatin blocks the G2/M phase of cell cycle. **d** Alteration of cell cycle related proteins by PD0166285 combined with cisplatin. *$p < 0.05$, **$p < 0.01$, ***$p < 0.001$

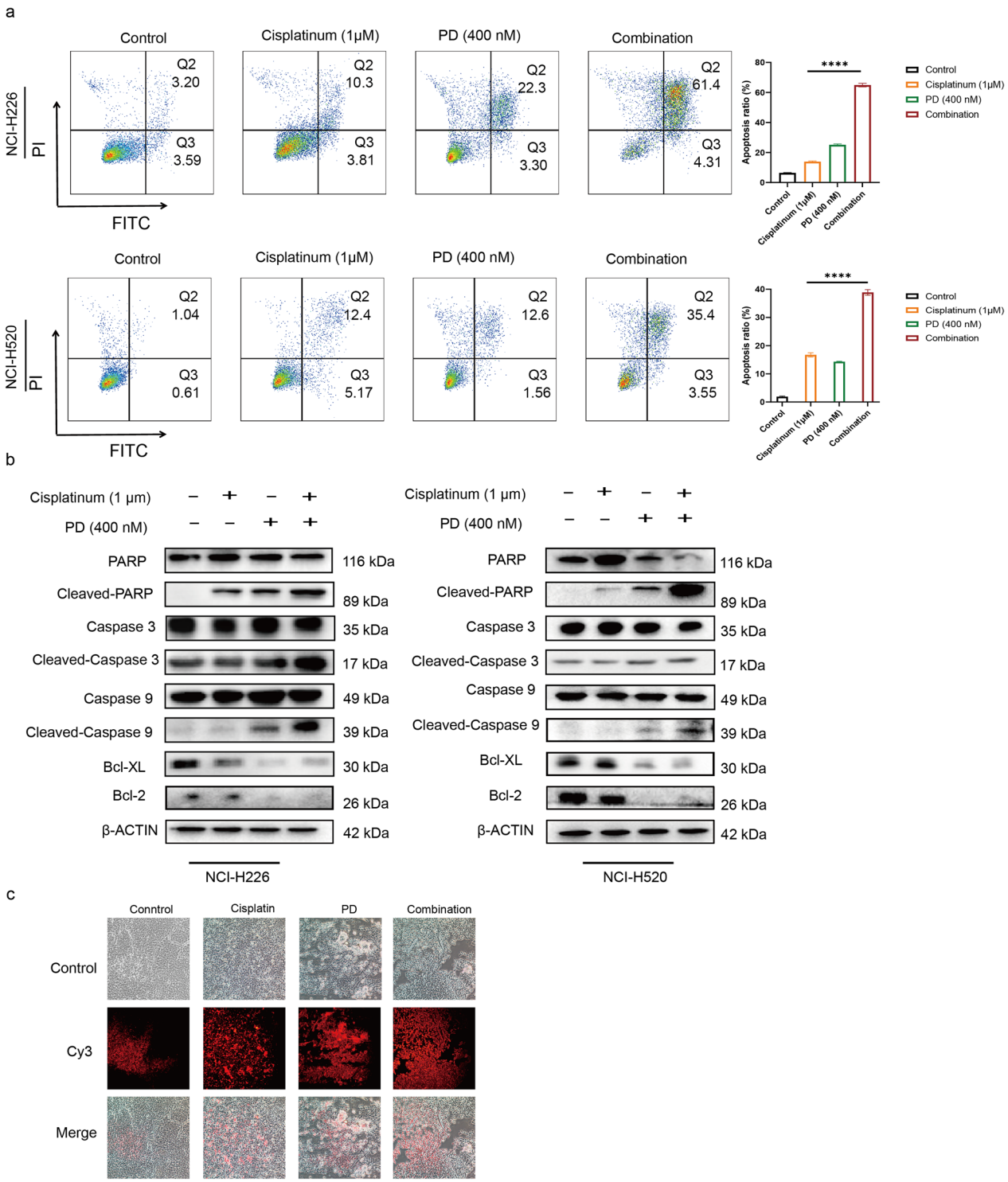

Fig. 5 Combination therapy of PD0166285 and cisplatin enhances apoptosis in LUSCs. **a** The combination of PD0166285 and cisplatin enhances the apoptosis ratio in LUSC tumor cells. **b** PD0166285 combined with cisplatin alters the protein levels of apoptosis-related proteins. **c** PD0166285 combined with cisplatin accelerates apoptosis in vivo. $^{*}p < 0.05$, $^{**}p < 0.01$, $^{***}p < 0.001$

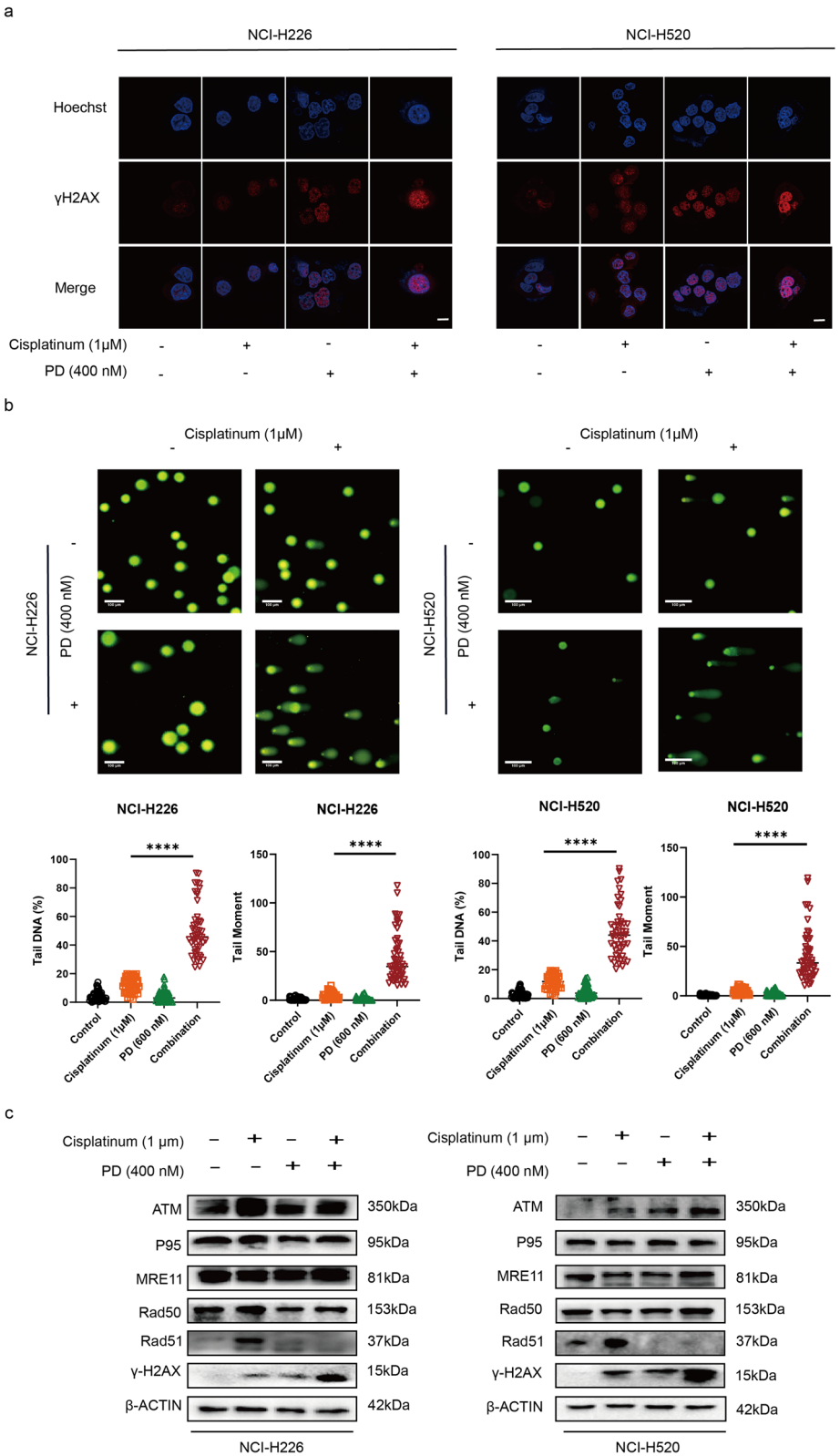

Fig. 6 PD0166285 enhances the DNA damage caused by cisplatin in LUSCs. **a** γ-H2AX foci increase following treatment with PD0166285 in combination with cisplatin. Scale bar = 10 μM. **b** Alkaline comet assay of LUSC tumor cells with control, cisplatin, PD0166285 alone and in combination with cisplatin. Comet tails and tail moments are measured in different groups. Scale bar = 100 μM. **c** PD0166285 modulates DNA damage repair through Rad51 in LUSCs. *$p < 0.05$, **$p < 0.01$, ***$p < 0.001$

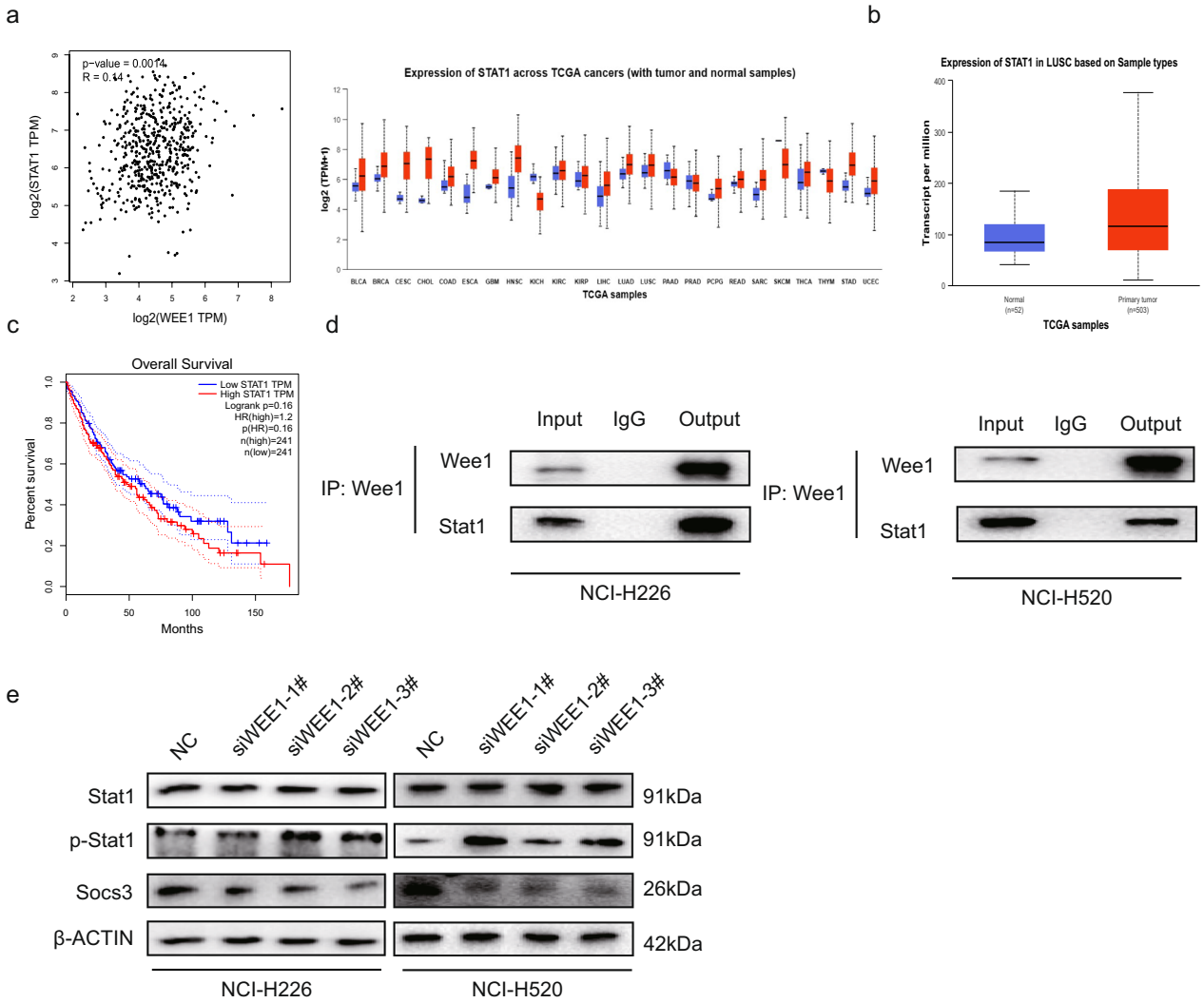

Fig. 7 PD0166285 interacts with Stat1 in LUSC tumor cells. **a, b, c** Wee1 interacts with Stat1. Stat1 is highly expressed in pan-cancer and tumor tissues. Stat1 is associated with poor prognosis. **d** Co-IP assay was performed to detect the interaction between Wee1 and Stat1 in LUSC. **e** p-Stat1 and Socs3 expression after knock-down of Wee1. $*p < 0.05$, $**p < 0.01$, $***p < 0.001$

the expression of Stat1 remained unchanged, while the expression of the p-Stat1 was up-regulated, while Socs3 was down-regulated. This indicates that the Stat1 signaling pathway is activated following Wee1 inhibition (Fig. 7e).

PD0166285 inhibits the growth and increases the chemosensitivity of LUSC to cisplatin in vivo

We established a nude mouse model using LUSCs cells. When the tumor size reached 100–150 mm^3, the nude mice were randomly assigned to different treatment groups: control (no treatment), cisplatin alone (5 mg/kg), PD0166285 alone (10 mg/kg), and combination therapy with cisplatin and PD0166285. Treatment with cisplatin plus PD0166285 demonstrated significantly enhanced suppression of tumor growth compared to either treatment alone (Fig. 8a). Western blot analysis of mouse tumor samples showed consistent results with our in vitro findings, with altered expression of Wee1, Phospho-Stat1, cleaved-PARP, Cyclin B, Rad51, Phospho-CDK1 T14, and phospho-CDK1 Y15 (Fig. 8b). To evaluate the toxicity of PD0166285, liver and kidney tissues were examined using hematoxylin and eosin (HE) staining, revealing no significant cellular damage (Fig. 8c). Immunohistochemical staining of LUSC tumor samples revealed upregulated expression levels of Phospho-Y15, γ-H2AX and Phospho-Stat1 (Fig. 8).

Discussion

The development of novel drugs for LUSC is highly challenging due to the complex tumor genomics and limited understanding of the oncogenic pathways [2]. Despite significant advancements in cancer therapeutics, including immunotherapy, effective treatments tailored for LUSC remain scarce, leaving patients with advanced-stage disease with limited therapeutic options [1]. In our recent study, we have shown that PD0166285, a Wee1 inhibitor, effectively disrupts the G2/M phase of the cell cycle. Moreover, when PD0166285 is used in combination with cisplatin, PD0166285 induces apoptosis. We investigated the underlying mechanisms of this combination therapy from two perspectives: first, PD0166285 combined with cisplatin induces DNA damage by decreasing the expression of Rad51 and causing mitotic catastrophe. Second, this combination therapy induces apoptosis via activation of the Stat1 pathway. Our study elucidates the specific mechanisms of PD0166285 in combination with cisplatin in the treatment of LUSC, providing an effective basis for optimizing therapeutic strategies for this challenging disease.

PD0166285 is the first drug reported to have inhibitory activity at low doses against Wee1, PKMYT1, and several other kinases including c-Src, EGFR, FGFR1, CHK1, and PDGFRβ [10]. Previous research indicated that the non-selective action of PD0166285 at low concentrations limited its therapeutic use. However, recent studies have demonstrated that combining PD0166285 with bortezomib selectively induces cell death in various types of solid tumor cells [40, 41]. In our studying, consistent with these findings, PD0166285, at nanomolar concentrations, effectively arrests cells at the G2 phase, inducing apoptosis in a time-dependent and concentration-dependent manner. Additionally, the combination of PD0166285 with cisplatin significantly showed synergistic effects. It is well established that the regulation of the G2 checkpoint is critical for *TP53*-mutant cells [42]. Recent studies demonstrate that WEE1 exhibits a significant synthetic lethal effect on *TP53*-mutated tumors [43, 44]. Unlike other Wee1 inhibitors, PD0166285's effectiveness appears to be correlated with the functional status of *TP53*, whereas AZD1775 inhibits Wee1 independent of *TP53* status [27, 29]. Our study also showed that PD0166285 was more effective in sensitizing *TP53*-deficient tumor cells [10, 45].

To investigate the mechanism of PD0166285 in inducing DNA damage, we conducted a series of assays. Wee1 is a critical protein kinase that regulates the G2/M cell cycle checkpoint, a pivotal stage in the cell cycle where DNA damage is assessed before cells enter mitosis [46]. Previous studies have shown that Wee1 inhibition markedly reduces the expression of Rad51, a protein involved in DNA damage repair [46, 47]. Consistent with these findings, our data also demonstrated a similar trend in LUSC. Rad51 is a member of the Rad52 epistasis group and plays a key role in homologous recombination (HR) and the maintenance of genomic stability [48, 49]. When treated with DNA-damaging agents, Rad51 is upregulated, further indicating its crucial role in HR [48]. Consistent with this, our experiments revealed a significant upregulation of Rad51 expression during cisplatin treatment. Additionally, we detected other proteins associated with DNA damage; however, the expression levels of these proteins remained unchanged. Therefore, further studies are needed to fully elucidate the mechanism by which Wee1 regulates Rad51.

In addition to inducing DNA damage, we found that the combination of PD0166285 with cisplatin significantly increased the rate of apoptosis. Analysis of data from The Cancer Genome Atlas (TCGA) revealed an interaction between Wee1 and Stat1, further validated through co-immunoprecipitation (CO-IP) assays. Stat1 plays a crucial role in regulating cell apoptosis and modulating the immune cell landscape [34]. Furthermore, a study has reported that tannic acid can increase the levels of phosphorylated Stat1 (p-Stat1), thereby enhancing apoptosis in breast cancer cells. This report suggested a potential mechanism by which PD0166285 and cisplatin may exert their effects [34]. Another study demonstrated that treatment with 1 μM AZD1775 significantly increased phosphorylated signal transducer and activator of p-Stat1 levels in small cell lung cancer (SCLC) cell lines [37]. We observed an upregulation of p-Stat1 upon inhibition of Wee1 in LUSC cell lines. Suppressors of cytokine signaling (SOCS) proteins serve as critical negative feedback regulators in cytokine signaling via the Janus kinase (JAK)-Stat pathway. Notably, SOCS1 and SOCS3 play pivotal roles in the development

(See figure on next page.)

Fig. 8 PD0166285 sensitizes the LUSC to cisplatin in vivo. **a** Inhibition of tumor growth in vivo following PD0166285 plus cisplatin treatment. **b** Expression analysis of Wee1, Stat1, Phospho-Stat1, cleaved-PARP, CyclinB, Rad51, Phospho-CDK1 T14 and Phospho-CDK1 Y15 in vivo after PD0166285 treatment. **c** Assessment of hepatorenal toxicity in vivo using HE staining. Scale bar = 200 μM in 5×. **d** IHC assay to demonstrate expression of Phospho-CDK1 Y15 and γ-H2AX after PD0166285 treatment. Scale bar = 50 μM in 20×, Scale bar = 25 μM in 40×. ns > 0.05, *$p < 0.05$, **$p < 0.01$, ***$p < 0.001$

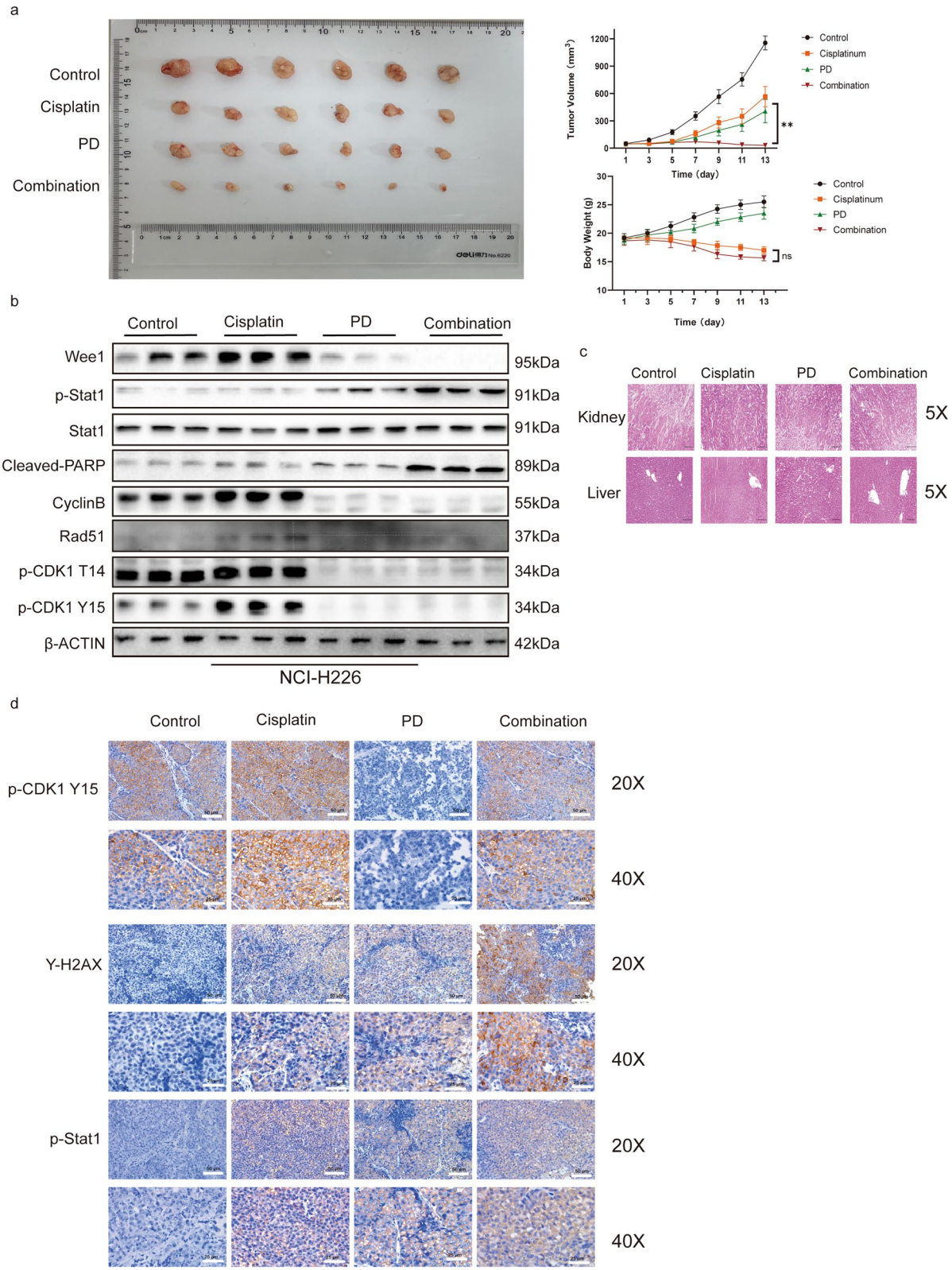

Fig. 8 (See legend on previous page.)

and progression of cancers [50, 51]. The Src homology 2 (SH2) domain competitively binds to phosphorylated tyrosine sites on cytokine receptors, thereby preventing Stat activation [52]. SOCS1 and SOCS2 play critical roles in regulating Stat3 and Stat5 activation, SOCS3 regulates additional Stat pathways including Stat1 and Stat4 [53–56]. In our studying, upon silencing the expression of Wee1, we observed activation of p-Stat1 and subsequent downregulation of SOCS3. Further investigation into the underlying mechanisms, particularly involving immune responses, is warranted.

Several clinical trials have developed Wee1 inhibitors. In Phase I and Phase II trials, PD0166285 in combination with carboplatin improved outcomes in advanced *TP53* mutant solid tumors [57]. PD0166285 targets both Wee1 and PKMYT1, making it a suitable pharmacological candidate for combination strategies in cancer treatment [10]. Some studies suggest that inhibition of Wee1 may enhance the cytotoxic effects of DNA-damaging drugs [58]. Among several DDR inhibitors, Wee1 inhibitors have been highlighted as particularly effective, demonstrating comparatively lower off-target toxicity [10]. In our analysis of liver and kidney toxicity in a mouse model, we observed that combination therapy resulted in low toxicity. Currently, numerous ongoing clinical trials are investigating combinations of Wee1 inhibitors with DNA damaging agents [40].

PD0166285 is notoriously promiscuous, not limiting its interaction with Wee1, which poses a challenge for its clinical application and is considered a limitation of this study. Consequently, future development efforts for Wee1 inhibitors will likely focus on optimizing their structural properties to address these challenges. Meanwhile, the mechanism of PD0166285 in immunity remains poorly understood and requires further detailed investigation.

In conclusion, our study reaffirms the sensitizing effect of PD0166285, underscoring the critical role of the G2/M checkpoint in cellular response to chemotherapy. These findings highlight Wee1 as a promising therapeutic target for future adjuvant therapy in *TP53*-mutated LUSC. Our results demonstrate that Wee1 responds to DNA damage through the Rad51 pathway and induces apoptosis via Stat1 activation. Additionally, we discovered an interaction between Wee1 and Stat1, offering a new direction for selecting drugs for combined immunotherapy in the future. Furthermore, the combination therapy of a Wee1 inhibitor and cisplatin significantly lowers the IC50 of cisplatin compared to monotherapy, demonstrating enhanced clinical efficacy and reduced toxicity, thereby providing a foundation for drug optimization. Importantly, our study addresses a gap in the research on Wee1 inhibitors in *TP53*-mutated LUCS, as there has been limited exploration of the functions of Wee1 and Stat1 in LUSC. Moving forward, further exploration of the interaction mechanism between Wee1 and Stat1 is warranted.

Acknowledgements
We thank Professor Ji Cao from the Zhejiang University School of Pharmacy and Dr. Xu Lin from the First Hospital affiliated of Zhejiang University School of Medicine for their invaluable technical support in both the selection of the research topic and the development of the experiment.

Author contributions
Qi Li made substantial contributions to conception and design, acquisition of data, and analysis and interpretation of data. Wenjie Yang performed the experiments and wrote the main manuscript text. Qingyi Zhang, Daoming Zhang, Jun Deng and Binxin Chen was involved in performing the experiments. Ping Li, Huanqi Zhang, Yiming Jiang and Yangling Li revised the article critically for important intellectual content; Bo Zhang and Nengming Lin had given final approval of the version to be published. All authors reviewed the manuscript.

Funding
This study was funded by National Natural Science Foundation of China (81702887, 82303515), Key Laboratory of Clinical Cancer Pharmacology and Toxicology Research of Zhejiang Province (2020E10021), Zhejiang Provincial Program for the Cultivation of High-level Innovative Health Talents (ZWB-2020-18), Zhejiang Medical Key Discipline Foundation (ZWB-2018-02-03), Hangzhou Medical Key Discipline Foundation (HWF-2021-21-16), Zhejiang Provincial Natural Science Foundation (LQ24H160024, LY21H160017), Science Research Foundation of Zhejiang Health Bureau (2020RC026).

Availability of data and materials
The datasets used and/or analyzed during the current study are available from the corresponding author on reasonable request. No datasets were generated or analysed during the current study.

Declarations

Ethics approval and consent to participate.
Every procedure was approved by the Hangzhou Medical College Experimental Animal Center, Hangzhou, China.

Consent for publication
Not applicable.

Competing interests
The authors declare that they have no competing interests.

Author details
[1]Department of Pharmacology, School of Basic Medical Sciences, Zhejiang University, Hangzhou 310058, China. [2]Key Laboratory of Clinical Cancer Pharmacology and Toxicology Research of Zhejiang Province, Hangzhou First People's Hospital, Hangzhou 310006, China. [3]The Fourth Clinical College of Zhejiang, First People's Hospital, Chinese Medicine University, Zhejiang Chinese Medical University, Hangzhou 310006, China. [4]Department of Thoracic Surgery, The First Affiliated Hospital, Zhejiang University School of Medicine, Hangzhou 310003, China. [5]Research Center for Clinical Pharmacy, College of Pharmaceutical Sciences, Zhejiang University, Hangzhou 310058, China. [6]Department of Pharmacy, The First Affiliated Hospital of Guangxi Medical University, Guangxi 530021, China. [7]College of Pharmaceutical Sciences, Zhejiang Chinese Medical University, Hangzhou 310053, China. [8]Key Laboratory of Clinical Cancer Pharmacology and Toxicology Research of Zhejiang Province, Affiliated Hangzhou First People's Hospital, Zhejiang University School of Medicine, Hangzhou 310006, China.

Received: 10 April 2024 Accepted: 21 August 2024
Published online: 13 September 2024

References

1. Niu Z, Jin R, Zhang Y, Li H. Signaling pathways and targeted therapies in lung squamous cell carcinoma: mechanisms and clinical trials. Signal Transduct Target Ther. 2022. https://doi.org/10.1038/s41392-022-01200-x.
2. Lau SCM, Pan Y, Velcheti V, Wong KK. Squamous cell lung cancer: current landscape and future therapeutic options. Cancer Cell. 2022;40(11):1279–93.
3. Herbst RS, Morgensztern D, Boshoff C. The biology and management of non-small cell lung cancer. Nature. 2018;553(7689):446–54.
4. Barta JA, Powell CA, Wisnivesky JP. Global epidemiology of lung cancer. Ann Global Health. 2019. https://doi.org/10.5334/aogh.2419.
5. Ruiz EJ, Diefenbacher ME, Nelson JK, Sancho R, Pucci F, Chakraborty A, Moreno P, Annibaldi A, Liccardi G, Encheva V, et al. LUBAC determines chemotherapy resistance in squamous cell lung cancer. J Exp Med. 2019;216(2):450–65.
6. Yin Y, Shen Q, Tao R, Chang W, Li R, Xie G, Liu W, Zhang P, Tao K. Wee1 inhibition can suppress tumor proliferation and sensitize p53 mutant colonic cancer cells to the anticancer effect of irinotecan. Mol Med Reports. 2017. https://doi.org/10.3892/mmr.2017.8230.
7. Van Linden AA, Baturin D, Ford JB, Fosmire SP, Gardner L, Korch C, Reigan P, Porter CC. Inhibition of Wee1 sensitizes cancer cells to antimetabolite chemotherapeutics In Vitro and In Vivo, independent of p53 functionality. Mol Cancer Ther. 2013;12(12):2675–84.
8. Zhou B-BS, Bartek J. Targeting the checkpoint kinases chemosensitization versus chemoprotection. Nat Rev Cancer. 2004;4(3):216–25.
9. Luo J, Solimini NL, Elledge SJ. Principles of cancer therapy: oncogene and non-oncogene addiction. Cell. 2009;136(5):823–37.
10. Luserna G, di Rorà A, Cerchione C, Martinelli G, Simonetti G. A WEE1 family business: regulation of mitosis, cancer progression, and therapeutic target. J Hematol Oncol. 2020. https://doi.org/10.1186/s13045-020-00959-2.
11. Hu Z, Li L, Lan W, Wei X, Wen X, Wu P, Zhang X, Xi X, Li Y, Wu L, et al. Enrichment of Wee1/CDC2 and NF-κB Signaling Pathway constituents mutually contributes to CDDP resistance in human osteosarcoma. Cancer Res Treat. 2022;54(1):277–93.
12. Yang X, Hu X, Yin J, Li W, Fu Y, Yang B, Fan J, Lu F, Qin T, Kang X, et al. Comprehensive multi-omics analysis reveals WEE1 as a synergistic lethal target with hyperthermia through CDK1 super-activation. Nat Commun. 2024. https://doi.org/10.1038/s41467-024-46358-w.
13. Zhu X, Su Q, Xie H, Song L, Yang F, Zhang D, Wang B, Lin S, Huang J, Wu M, et al. SIRT1 deacetylates WEE1 and sensitizes cancer cells to WEE1 inhibition. Nat Chem Biol. 2023;19(5):585–95.
14. Matheson CJ, Venkataraman S, Amani V, Harris PS, Backos DS, Donson AM, Wempe MF, Foreman NK, Vibhakar R, Reigan P. A WEE1 inhibitor analog of AZD1775 maintains synergy with cisplatin and demonstrates reduced single-agent cytotoxicity in medulloblastoma cells. ACS Chem Biol. 2016;11(7):2066–7.
15. Leijen SBJ, Schellens JH. Abrogation of the G2 checkpoint by inhibition of Wee-1 kinase results in sensitization of p53-deficient tumor cells to DNA-damaging agents. Curr Clin Pharmaco. 2010;5:186–91.
16. Santo L, Siu KT, Raje N. Targeting cyclin-dependent kinases and cell cycle progression in human cancers. Semin Oncol. 2015;42(6):788–800.
17. Benada J, Macurek L. Targeting the checkpoint to kill cancer cells. Biomolecules. 2015;5(3):1912–37.
18. De Witt Hamer PC, Mir SE, Noske D, Van Noorden CJF, Würdinger T. WEE1 kinase targeting combined with DNA-damaging cancer therapy catalyzes mitotic catastrophe. Clin Cancer Res. 2011;17(13):4200–7.
19. Bridges KA, Hirai H, Buser CA, Brooks C, Liu H, Buchholz TA, Molkentine JM, Mason KA, Meyn RE. MK-1775, a Novel Wee1 kinase inhibitor, radiosensitizes p53-defective human tumor cells. Clin Cancer Res. 2011;17(17):5638–48.
20. Cancer Genome Atlas Research Network. Comprehensive molecular profiling of lung adenocarcinoma. Nature. 2014;511(7511):543–50.
21. Heist RS, Sequist LV, Engelman JA. Genetic changes in squamous cell lung cancer: a review. J Thorac Oncol. 2012;7(5):924–33.
22. Lan H, Tan M, Zhang Q, Yang F, Wang S, Li H, Xiong X, Sun Y. LSD1 destabilizes FBXW7 and abrogates FBXW7 functions independent of its demethylase activity. Proc Natl Acad Sci. 2019;116(25):12311–20.
23. Lafay-Cousin L, Purdy E, Huang A, Cushing SL, Papaioannou V, Nettel-Aguirre A, Bouffet E. Early cisplatin induced ototoxicity profile may predict the need for hearing support in children with medulloblastoma. Pediatr Blood Cancer. 2012;60(2):287–92.
24. Mir SE, De Witt Hamer PC, Krawczyk PM, Balaj L, Claes A, Niers JM, Van Tilborg AAG, Zwinderman AH, Geerts D, Kaspers GJL, et al. In silico analysis of kinase expression identifies WEE1 as a gatekeeper against mitotic catastrophe in glioblastoma. Cancer Cell. 2010;18(3):244–57.
25. Hashimoto O, Shinkawa M, Torimura T, Nakamura T, Selvendiran K, Sakamoto M, Koga H, Ueno T, Sata M. Cell cycle regulation by the Wee1 Inhibitor PD0166285, Pyrido [2,3-d] pyimidine, in the B16 mouse melanoma cell line. BMC Cancer. 2006. https://doi.org/10.1186/1471-2407-6-292.
26. Hashimoto O, Ueno T, Kimura R, Ohtsubo M, Nakamura T, Koga H, Torimura T, Uchida S, Yamashita K, Sata M. Inhibition of proteasome-dependent degradation of Wee1 in G2-arrested Hep3B cells by TGFβ1. Mol Carcinog. 2003;36(4):171–82.
27. Matheson CJ, Backos DS, Reigan P. Targeting WEE1 kinase in cancer. Trends Pharmacol Sci. 2016;37(10):872–81.
28. Yan J, Zhuang L, Wang Y, Jiang Y, Tu Z, Dong C, Zhu Y. Inhibitors of cell cycle checkpoint target Wee1 kinase—a patent review (2003–2022). Expert Opin Ther Pat. 2023;32(12):1217–44.
29. Kong A, Mehanna H. WEE1 Inhibitor: clinical development. Curr Oncol Reports. 2021. https://doi.org/10.1007/s11912-021-01098-8.
30. PosthumaDeBoer J, Würdinger T, Graat HCA, van Beusechem VW, Helder MN, van Royen BJ, Kaspers GJL. WEE1 inhibition sensitizes osteosarcoma to radiotherapy. BMC Cancer. 2011. https://doi.org/10.1186/1471-2407-11-156.
31. Lee Y-Y, Cho Y-J, Shin S-W, Choi C, Ryu J-Y, Jeon H-K, Choi J-J, Hwang JR, Choi CH, Kim T-J, et al. Anti-tumor effects of Wee1 kinase inhibitor with radiotherapy in human cervical cancer. Sci Reports. 2019. https://doi.org/10.1038/s41598-019-51959-3.
32. da Costa AABA, Chowdhury D, Shapiro GI, D'Andrea AD, Konstantinopoulos PA. Targeting replication stress in cancer therapy. Nat Rev Drug Discovery. 2022;22(1):38–58.
33. Wang W, Lopez McDonald MC, Kim C, Ma M, Pan Z, Kaufmann C, Frank DA. The complementary roles of STAT3 and STAT1 in cancer biology: insights into tumor pathogenesis and therapeutic strategies. Front Immunol. 2023. https://doi.org/10.3389/fimmu.2023.1265818.
34. Wong GL, Manore SG, Doheny DL, Lo H-W. STAT family of transcription factors in breast cancer: pathogenesis and therapeutic opportunities and challenges. Semin Cancer Biol. 2022;86:84–106.
35. Zeng Y, Chen H-Q, Zhang Z, Fan J, Li J-Z, Zhou S-M, Wang N, Yan S-P, Cao J, Liu J-Y, et al. IFI44L as a novel epigenetic silencing tumor suppressor promotes apoptosis through JAK/STAT1 pathway during lung carcinogenesis. Environ Pollut. 2023. https://doi.org/10.1016/j.envpol.2022.120943.
36. Zhang H, Zhu C, He Z, Chen S, Li L, Sun C. LncRNA PSMB8-AS1 contributes to pancreatic cancer progression via modulating miR-382–3p/STAT1/PD-L1 axis. J Exp Clin Cancer Res. 2020. https://doi.org/10.1186/s13046-020-01687-8.
37. Taniguchi H, Caeser R, Chavan SS, Zhan YA, Chow A, Manoj P, Uddin F, Kitai H, Qu R, Hayatt O, et al. WEE1 inhibition enhances the antitumor immune response to PD-L1 blockade by the concomitant activation of STING and STAT1 pathways in SCLC. Cell Rep. 2022. https://doi.org/10.1016/j.celrep.2022.110814.
38. Alexandre AB, da Costa A, Chowdhury D, Shapiro GI, D'Andrea AD, Konstantinopoulos PA. Targeting replication stress in cancer therapy. Nat Rev Drug Discov. 2023;22(1):38–58.
39. Chen D, Lin X, Gao J, Shen L, Li Z, Dong B, Zhang C, Zhang X. Wee1 inhibitor AZD1775 combined with cisplatin potentiates anticancer activity against gastric cancer by increasing DNA damage and cell apoptosis. Biomed Res Int. 2018;2018:1–10.
40. Bukhari AB, Chan GK, Gamper AM. Targeting the DNA damage response for cancer therapy by inhibiting the kinase Wee1. Front Oncol. 2022. https://doi.org/10.3389/fonc.2022.828684.
41. Chen Z-L, Xie C, Zeng W, Huang R-Q, Yang J-E, Liu J-Y, Chen Y-J, Zhuang S-M. Synergistic induction of mitotic pyroptosis and tumor remission by inhibiting proteasome and WEE family kinases. Signal Transduct Target Ther. 2024. https://doi.org/10.1038/s41392-024-01896-z.
42. Li S, Juengpanich S, Topatana W, Xie T, Hou L, Zhu Y, Chen J, Shan Y, Han Y, Lu Z, et al. Adavosertib-encapsulated metal-organic frameworks for p53-mutated gallbladder cancer treatment via synthetic lethality. Sci Bull. 2024;69(9):1286–301.

43. Méndez E, Rodriguez CP, Kao MC, Raju S, Diab A, Harbison RA, Konnick EQ, Mugundu GM, Santana-Davila R, Martins R, et al. A Phase I clinical trial of AZD1775 in combination with neoadjuvant weekly docetaxel and cisplatin before definitive therapy in head and neck squamous cell carcinoma. Clin Cancer Res. 2018;24(12):2740–8.
44. Diab A, Kao M, Kehrli K, Kim HY, Sidorova J, Mendez E. Multiple defects sensitize p53-deficient head and neck cancer cells to the WEE1 kinase inhibition. Mol Cancer Res. 2019;17(5):1115–28.
45. Al-Jamaei AH, de Visscher JGAM, Subramanyam VR, Forouzanfar T, Sminia P, Doulabi BZ, Helder MN. WEE1 kinase inhibitor MK-1775 sensitizes oral tongue squamous cell carcinoma cells to radiation irrespective of TP53 status. Oral Dis. 2022;29(7):2640–9.
46. Fukuda K, Takeuchi S, Arai S, Nanjo S, Sato S, Kotani H, Kita K, Nishiyama A, Sakaguchi H, Ohtsubo K, et al. Targeting WEE1 enhances the antitumor effect of KRAS-mutated non-small cell lung cancer harboring TP53 mutations. Cell Reports Med. 2024. https://doi.org/10.1016/j.xcrm.2024.101578.
47. Zeng F, Peng Y, Qin Y, Wang J, Jiang G, Feng W, Yuan Y. Wee1 promotes cell proliferation and imatinib resistance in chronic myeloid leukemia via regulating DNA damage repair dependent on ATM-γH2AX-MDC1. Cell Commun Signal. 2022. https://doi.org/10.1186/s12964-022-01021-z.
48. Myers SH, Ortega JA, Cavalli A. Synthetic lethality through the lens of medicinal chemistry. J Med Chem. 2020;63(23):14151–83.
49. Bhowmick R, Lerdrup M, Gadi SA, Rossetti GG, Singh MI, Liu Y, Halazonetis TD, Hickson ID. RAD51 protects human cells from transcription-replication conflicts. Mol Cell. 2022;82(18):3366-3381.e3369.
50. Han Q, Zhou H, Xie W, Sun T, Wei R, Nie C, Hong J, Zhu L, Tian W. Association between the methylation of the STAT1 and SOCS3 in peripheral blood and gastric cancer. J Gastroenterol Hepatol. 2020;35(8):1347–54.
51. Jiang M, Zhang W-W, Liu P, Yu W, Liu T, Yu J. Dysregulation of SOCS-mediated negative feedback of cytokine signaling in carcinogenesis and its significance in cancer treatment. Front Immunol. 2017;8:70.
52. Masuzaki R, Kanda T, Sasaki R, Matsumoto N, Nirei K, Ogawa M, Karp SJ, Moriyama M, Kogure H. Suppressors of cytokine signaling and hepatocellular carcinoma. Cancers. 2022. https://doi.org/10.3390/cancers14102549.
53. Zhou J, Li Z, Wu T, Zhao Q, Zhao Q, Cao Y. LncGBP9/miR-34a axis drives macrophages toward a phenotype conducive for spinal cord injury repair via STAT1/STAT6 and SOCS3. J Neuroinflammation. 2020;17(1):134.
54. Lang R, Pauleau A-L, Parganas E, Takahashi Y, Mages J, Ihle JN, Rutschman R, Murray PJ. SOCS3 regulates the plasticity of gp130 signaling. Nat Immunol. 2003;4:546–50.
55. Peng HY, Jiang SS, Hsiao JR, Hsiao M, Hsu YM, Wu GH, Chang WM, Chang JY, Jin SL, Shiah SG. IL-8 induces miR-424-5p expression and modulates SOCS2/STAT5 signaling pathway in oral squamous cell carcinoma. Mol Oncol. 2016;10(6):895–909.
56. Chan SR, Rickert CG, Vermi W, Sheehan KC, Arthur C, Allen JA, White JM, Archambault J, Lonardi S, McDevitt TM, et al. Dysregulated STAT1-SOCS1 control of JAK2 promotes mammary luminal progenitor cell survival and drives ERalpha(+) tumorigenesis. Cell Death Differ. 2014;21(2):234–46.
57. Benada J, Bulanova D, Azzoni V, Petrosius V, Ghazanfar S, Wennerberg K, Sørensen Claus S. Synthetic lethal interaction between WEE1 and PKMYT1 is a target for multiple low-dose treatment of high-grade serous ovarian carcinoma. NAR Cancer. 2023. https://doi.org/10.1093/narcan/zcad029.
58. Gourley C, Balmaña J, Ledermann JA, Serra V, Dent R, Loibl S, Pujade-Lauraine E, Boulton SJ. Moving from poly (ADP-Ribose) polymerase inhibition to targeting DNA repair and DNA damage response in cancer therapy. J Clin Oncol. 2019;37(25):2257–69.

Publisher's Note